

Mahanth Gowda Pennsylvania State University

Ashutosh Dhekne*, Sheng Shen* and Romit Roy Choudhury University of Illinois at Urbana-Champaign

Sharon Xue Yang, Lei Yang, Suresh Golwalkar and Alexander Essanian Intel

*Co-secondary authors

Editors: Aruna Balasubramanian and Lin Zhong



IoT PLATFORMS FOR SPORTS ANALYTICS

This paper is an experience report on IoT platforms for sports analytics. In our prior work [11], we proposed *iBall*, a system that explores the possibility of bringing IoT to sports analytics, particularly to the game of Cricket. iBall develops solutions to track a ball's 3D trajectory and spin with inexpensive sensors and radios embedded in the ball. Towards this end, iBall performs fusion of wireless and inertial sensory data and integrates them into physics-based motion models of a ball in flight. The median ball location error is at 8cm while rotational error remains below 12° even at the end of the flight. The results do not rely on training, hence we expect the core techniques to extend to other sports like baseball, with some domain-specific modifications.

IoT-based analytics for sports has several applications. Patterns of balls, racquets, and players are being analyzed for coaching, strategic insights, and predictions. iBall provides a significantly cheaper alternative to million dollar camera-based solutions. Real-time analytics should be possible anytime, anywhere. Aspiring players in local clubs could read out their own performance from their smartphone screens; school coaches could offer quantifiable feedback to their students.

In this paper, we elaborate on our experience in developing iBall's IoT platform

– particularly on details from early ball prototyping, ground truth extraction and the technical platform. This includes several challenges in system design and engineering to satisfy various requirements of sensor embedding, impact resistance, high sampling rate, sensor calibration, synchronization, etc. iBall considers a case study of cricket ball tracking. However, the platform is also applicable to tracking other sporting objects (racquet, puck, hollow balls) and humans, with application-specific customization.

The rest of the paper is organized into three modules. We first discuss embedding of sensors inside cricket balls. Then we deliberate on various alternatives for obtaining ground truth for validating iBall's tracking algorithms. Finally, we discuss pre-processing steps necessary to work with sensor data from Inertial Measurement Units (IMU) and UltraWideBand (UWB) radios.

BALL PROTOTYPING

Figure 1 shows our sensor platform, which consists of a CPU, IMU and a UWB Radio. The IMU and UWB sensors provide measurements necessary for tracking the location and rotation of a ball. Embedding the platform inside a cricket ball is a non-trivial task and involves several engineering challenges. We worked with D2M [1], a mechanical design company towards this end. Below, we enumerate requirements for embedding the sensor.

Snugness: The sensor has to fit snugly inside the ball to avoid rattling and to capture the motion of the ball precisely.

Battery Life and Recharge-ability: The battery life of the sensor should support multiple hours of play before recharge. The battery should be accessible for charging. Design for wireless charging or energy harvesting should be considered.

Mass Distribution: An embedded sensor should not alter the mass distribution, so the aerodynamic properties of the ball will be kept unaffected.

Absorbing Impacts: The sensor should be able to withstand severe impacts generated when the ball is bounced or hit with a bat.

We now discuss some of the key designs explored towards satisfying these requirements.

Embedding in Wooden Core

We cut open an off-the-shelf cricket ball to access the wooden core as shown in Figure 2. A small section is then scooped out of the core, such that a plastic case holding the sensor (Figure 3) fits inside the cavity. A view of the case inside the ball is shown in Figure 4(a). Finally, the top of the wooden core is sealed using screws and the lid is closed and taped, to render a usable prototype, as shown in Figure 4(b). While the prototype couldn't withstand impacts, we could conduct several experiments without bouncing the ball. We conduct experiments to characterize the motion of the ball under flight. We also observe the impacts recorded by the accelerometer during throws, centripetal forces, angular velocities under spin, spin rate, magnetometer variations, etc. Properties of the unreactive accelerometer under free fall, gyroscope saturation under high spin as well as parabolic nature of trajectories were studied. The insights gathered form the core of tracking algorithms in iBall [11].

Embedding in 3D Printed Plastic Core

While the wooden core prototype provides valuable insights about the inertial properties of a cricket ball under flight, the flexibility for carving out finer structures with high precision is limited. We therefore consider an alternative as shown in Figure 5 with a 3D printed plastic core. This allows carving out smaller spaces for precisely embedding LEDs inside the ball for ground truthing (details in Section "LED Markers"). In addition, the plastic core offers another advantage. The screws and nuts used to attach various parts of the core lose traction

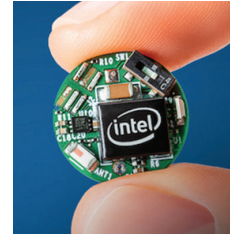


FIGURE 1. Intel Curie board.



FIGURE 2. Space carved out of the wooden core for sensor embedding.



FIGURE 3. Curie sensor embedded within a case.

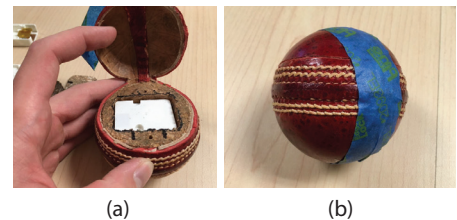


FIGURE 4. Sensor-embedded case fit into the ball (a). Sealed ball with the sensor (b).

(after a few cycles of operation) with the wooden core (Figure 2). The plastic core, on the other hand, maintains good traction. However, the main disadvantage is that the structural property of the ball, such as deformation during impact, is not maintained and the ball can break easily. For reasons mentioned in Section “LED Markers,” we decide not to pursue LEDs and hence we experiment with wooden core prototypes.

Handling Impact: Shock Absorbers

One of the main drawbacks of earlier prototypes is that they were not able to resist the impact of the ball with the ground. Hence, we embedded the sensor inside a shock-absorbent orange silicone rubber as shown in Figure 6. We then embedded it into the ball as in Figure 7. This prototype turned out to be more robust with ground impacts and was used for evaluation in iBall.

Summary and Future Considerations

The prototypes could snugly fit the sensors inside and offer a couple of hours of battery life. We could conduct experiments, collect data and design algorithms to track the location and rotation of the ball. However, the prototypes alter the mass distribution. Also, we did not test for impact resistance when hit with the bat. Experts from D2M [1] have corroborated that a near-ideal mass distribution with impact tolerance is feasible. The opportunities arise from the feasibility of reducing the spatial footprint of the sensor. Additionally, energy harvesting techniques could eliminate the battery altogether. Having a special-purpose computing platform instead of a general-purpose platform can also help in reducing the sensor size. A characterization of these designs is left for future work.



FIGURE 6. A shock-absorbing silicone rubber is used to wrap the sensor before embedding it inside a case.



FIGURE 5. A 3D-printed core offers more flexibility for precisely embedding tiny LEDs inside the ball.

GROUND TRUTH

A high-precision ground truth with mm level accuracy is necessary to validate iBall’s tracking algorithms. Designing such a platform is non-trivial because of the small size and high-speed motion of the ball, which makes it difficult to track. Below, we discuss various alternatives considered and associated tradeoffs.

LED Markers

We explore LED-based Motion Capturing (MOCAP) system from PhaseSpace [7]. Figure 8 shows the architecture of PhaseSpace MOCAP. A group of LED markers are placed on the target to be tracked. Each marker is uniquely identifiable and is tracked by multiple synchronized cameras. This results in a mm level accuracy in rotation and location estimates.

To derive LED based ground truth, we instrument the ball with LED markers. Figure 9 shows an example. While this was helpful, the protruding LEDs can make the ball unbouncable. Hence, we attempted to embed LEDs inside the ball

as shown in Figure 5. However, the effort was unsuccessful since the internal LEDs were occluded by the depth of the outer leather layer that covers the plastic core. Moreover, LEDs require that a controller is also embedded inside the ball to power and control them. This substantially increases the footprint of the infrastructure embedded and significantly alters the aerodynamic properties of the ball. Hence, we eliminate LEDs as a candidate and look for other alternatives.

Infrared Markers

A set of passive markers are placed on the object to be tracked. These markers reflect infrared light that is trackable by cameras (similar to tracking of active LEDs). However, unlike LEDs, the passive infrared markers do not have uniquely distinguishable identifiers. They are identified based on their relative geometry. The location of individual markers can be translated into 3D location and rotation of the ball similar to LED-based tracking.

First, we stuck infrared reflective tapes



FIGURE 7. Impact-absorbing sensor case is fit into the ball and then sealed.

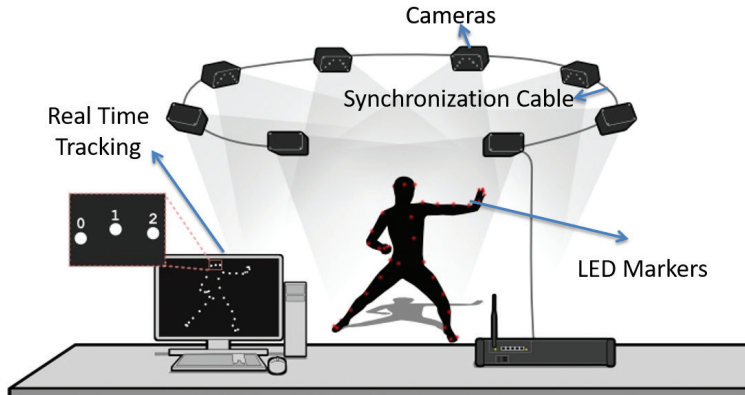


FIGURE 8. Motion Capture System (borrowed from [7]).

on the ball (see Figure 10) and attempted to track them with ViCON [5] infrared cameras. Sticky tapes can minimize the impact on the aerodynamics of the ball. However, since reflections are not strong, tracking is difficult. Hence, we had to stick spherical markers on the ball (see Figure 11), ultimately trading off ball aerodynamics for accuracy.

High-Speed Camera

High-speed visual cameras provide yet another alternative for ground truth measurements. Hawkeye[3] is a high-speed camera-based technology being used in professional games like cricket, tennis, soccer, etc., to track the location of a ball with mm level accuracy. However, Hawkeye cannot track the rotation of the ball, which is a key parameter for analytics.

We attempt to capture the rotation of the ball by sticking colored tape on the ball as shown in Figure 12(a). Figure 12(b) shows an experiment in which the color-taped ball is in flight and we wish to track its orientation using these tapes. Figure 12(c) is a close-up of the ball in flight. We attempt to determine the 3D rotation necessary to make the tapes parallel to the axes of the camera. In Figure 12(d), the ball has been visually rotated such that the tapes are aligned with the direction of camera axes. In sum, detecting the orientation of color tapes determines the orientation of the ball. Although the accuracy was reasonable, multiple cameras positioned close to the ball are necessary for tracking. Also, bright lighting conditions or outdoor infrastructure under sunlight is necessary to minimize blur from the high speed motion

of the ball. This substantially increases the complexity of the infrastructure. Although the camera has an advantage of being completely passive and not affecting the aerodynamics of the ball, we discarded it because of the above-mentioned drawbacks.

As discussed in Section “Infrared Markers,” we use the ViCON platform with spherical markers (Figure 11) for validating iBall.

TECHNICAL PLATFORM

The primary technical platform building iBall is composed of IMU sensors and UWB radios. IMU is used for tracking rotation and UWB is used for tracking location. In this section, we elaborate on the pre-processing steps necessary to work with the sensor data.

IMU

Calibration

An IMU consists of an accelerometer, gyroscope and magnetometer. More details on the operation and physical models can be found in [4]. The sensors measurements would invariably be noisy [10]. Some of these errors arise due to manufacturing imperfections, due to misalignment of sensor axes or internal effects, such as interference from the circuitry leading to biases and erroneous transformations on the measurements [8, 9]. While smartphone operating systems such as Android/iOS [6] might compensate the raw measurements for such artifacts before passing on the sensor data to a developer, a raw sensor hardware used in iBall needs systematic calibration. Below, we present a simplistic model of errors and techniques for compensation.



(a) (b)

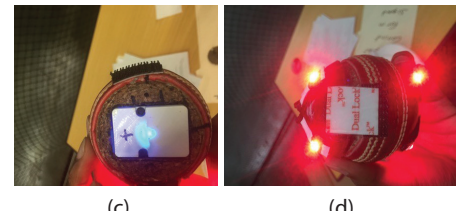


FIGURE 9. LED-instrumented ball (a). Sensor embedded inside (b). LEDs stuck with Velcro on the outside and sealed (c) LEDs powered (d).



FIGURE 10. A cricket ball instrumented with IR tapes.



FIGURE 11. A cricket ball instrumented with spherical IR markers.

Magnetometer: A magnetometer would measure the magnetic field vector as experienced by the sensor. In an environment free of magnetic interference, a magnetometer would measure the geomagnetic field. The magnitude of the measurement would be a constant at a given geographical location whereas the direction would be a function of sensor orientation. The measurement

would point towards the direction of the geomagnetic field relative to the sensor's frame of reference.

Given constant magnitude, the measurements of the geomagnetic field across different sensor orientation should lie on the surface of a zero centered sphere. However, in reality, sensor imperfections (e.g., axes misalignment, sensor misalignment, bias) pollute the measurements. A simple model of magnetometer error is expressed below.

$$Bx = sxHx + bx + \epsilon_x \quad (1)$$

Here, Bx is the x component of sensor measurement. Hx is the true x component of the magnetic field. sx corresponds to scale error, bx is a constant bias and ϵ_x is Gaussian noise. y and z components are also polluted by similar errors.

Due to scale and bias errors, measurements of the geomagnetic field across different orientations do not lie on a zero centered sphere. Instead, they lie on a non-zero centered ellipsoid as shown in Figure 13(a). The axes of this ellipsoid vary roughly by 5% (hence difficult to perceive the difference visually). We follow a simple ellipsoid fitting method as outlined in [2] to compute the scale and bias errors. The resulting sphere after compensation is plotted in Figure 13(b), which is a zero centered sphere. We apply the computed scale and bias corrections to all magnetometer measurements.

Accelerometer: An accelerometer also suffers from axes misalignment, scale and bias errors, like a magnetometer. Hence, the entire process of error modeling and compensation is similar. Figure 14 shows measurements of gravity at 10 different orientations of the accelerometer. Clearly,

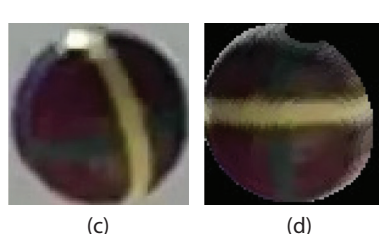
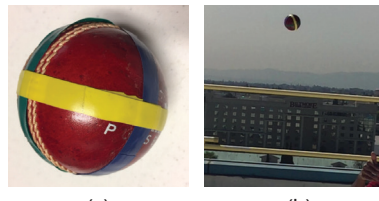


FIGURE 12. Tracking the 3D rotation of a ball visually using color tapes. Color-taped cricket ball (a). Ball in flight (b). Zoomed view of randomly oriented colored tapes (c). Visual alignment of tapes to camera axes (d).

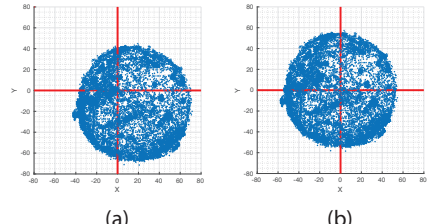


FIGURE 13. (a) Uncalibrated magnetometer samples – lie on a non zero centered ellipsoid. (b) Calibrated magnetometer samples – lie on a zero centered sphere.

Figure 17 shows the results for the previous experiment after compensating for the gyroscope bias. Evidently, the difference between final and initial orientations has been substantially reduced after bias compensation.

Synchronization with ViCon

To compare IMU data with ViCON, we need to synchronize the two frames to eliminate the offsets between their clocks. Towards this end, we begin data collection sessions with a synchronization phase. We hold the ball firmly in hand (with its Z-axis pointing to our right) and lower the arm down and up four times. During this period, ViCON records the ball moving down and up four times, while the gyroscope records the ball having negative-then-positive rotation around its own Z-axis four times. When the ball reaches the lowest point, ViCon's Z-axis data reaches minimum while gyroscopes Z-axis data crosses 0 and further goes up (Figure 18). We align these two sets of timestamps in the two systems to synchronize ViCon and the IMU sensor.

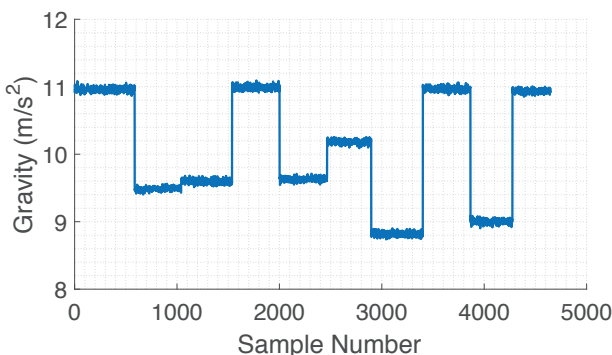


FIGURE 14. Gravity measurement with an uncalibrated accelerometer is error prone – a function of orientation.

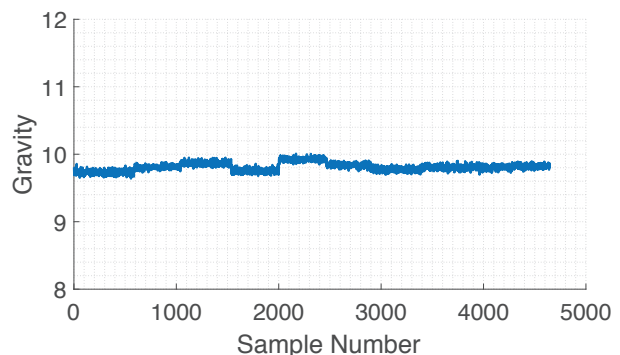


FIGURE 15. Gravity measurement from a calibrated accelerometer is close to 9.8 m/s^2 and independent of orientation.

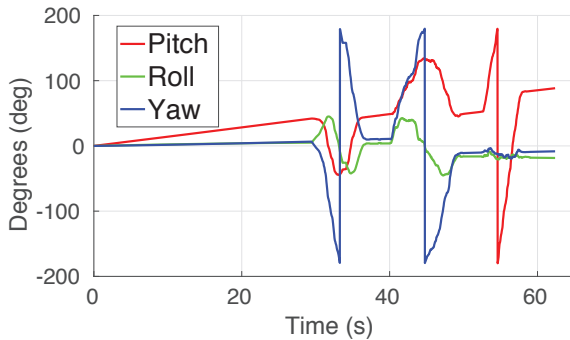


FIGURE 16. With an uncalibrated gyroscope, the error accumulates faster.

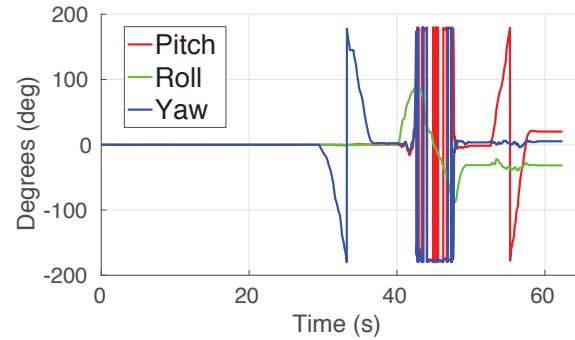


FIGURE 17. A calibrated gyroscope can decrease the error accumulation considerably.

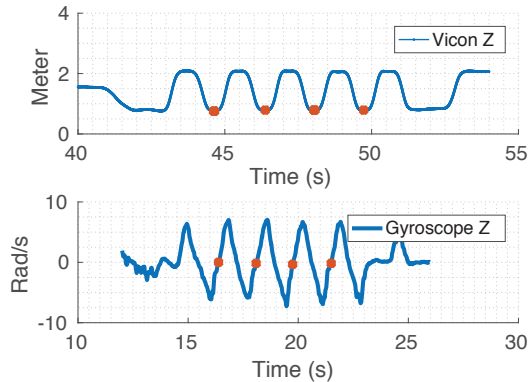


FIGURE 18. Matching minimas ViCON's z location with zero crossings of gyroscope's z-axis for synchronization.

Figure 18 shows the selection of these two sets of timestamps. By matching the highlighted points, the clocks can be synchronized to millisecond level accuracy.

UWB

iBall uses a UWB platform for localization. Two UWB radios (called anchors) are deployed on either end of the cricket pitch (stumps) as shown in Figure 19. The ball is also embedded with a UWB radio, capable of exchanging signals with the anchors. The anchors can measure their distance (Range) from the ball as well as Angle of Arrival of incoming signals, for localization. We elaborate on sampling rate and synchronization-related enhancements, which are critical to iBall's performance.

Enhancing the Sampling Rate

High-speed localization entails a high sampling rate of ranging measurements at the anchor. Briefly, each range measurement requires a “poll” message from the anchor

and a “response” packet from the ball. The range is then computed based on time of arrival of the response packet relative to the time at which the poll packet was sent. We need ranging measurements at both anchors for 3D localization. Naively extending the simple ranging scheme to multiple anchors will introduce two issues:

- (1) Since each anchor needs to perform ranging separately, sampling rate is reduced by a factor equal to the number of anchors
- (2) Time synchronization needs to be achieved offline between data from multiple anchors.

We follow a simple, yet effective, procedure to sidestep the above problems. Wireless signals pass through a broadcast medium. As illustrated in Figure 20, the poll and response packets initiated by one (Active) anchor can be overheard at another (passive anchor). By recording the time

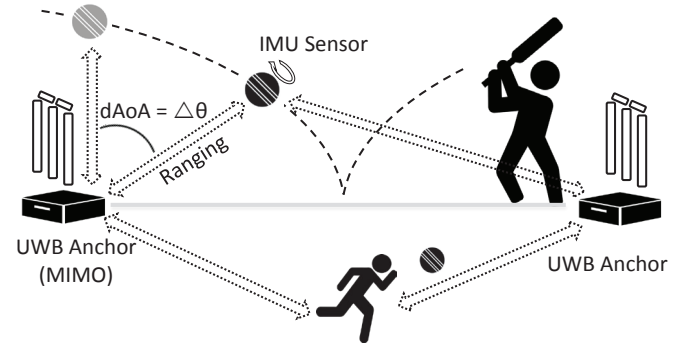


FIGURE 19. Two anchors and a ball deployed on the ground.

of arrival of these two packets, the passive anchor is able to automatically infer its range from the ball.

To validate such a passive ranging, we conduct an experiment, in which the ball performs a poll/response ranging with an active anchor. The range of the ball relative to that anchor is plotted in Figure 21(a) and compared with ViCON ground truth. A passive anchor deployed in the same area was also able to infer its range relative to the ball without any active transmissions of its own. Figure 21(b) shows that the passive range is in close agreement with ViCON ground truth. Also, passive ranging data is implicitly time synchronized with active ranging data since passive ranges are inferred from the same packets.

Synchronization with ViCON

Similar to IMU's synchronization with ViCON, the UWB's clock must also be synchronized with ViCON so as to compare UWB determined location with

ViCON. We follow a similar procedure as IMU synchronization discussed in Section “Synchronization with ViCon.”

CONCLUSION

This paper discusses our experience in developing an IoT-based platform for cricket ball tracking. A sensor embedded inside the ball should be snugly fit, impact resistant and should not hamper the ideal mass distribution of the ball. We consider various alternatives, including embeddings within a wooden core and 3D-printed plastic core. We use a rubber cushion for impact resistance. While not perfect, the prototype is stable enough to experiment with various speed and spin regimes offering valuable insights as reported in [11]. A high-precision ground truth is needed for benchmarking the tracking algorithms. While LED, ViCON and high-speed cameras offer unique tradeoffs, the right choice would be a function of a specific sport, mobility regimes and the range of coverage. Finally, working with the IMU sensor data as well as UWB measurements entails appropriate preprocessing steps, such as calibration, synchronization, sampling rate enhancements before using them for ball tracking. While there are opportunities to make the platform more robust and extensive, we believe there are many other sports analytics applications that can benefit with the platform. ■

Mahanth Gowda is an Assistant Professor in the CSE department at Pennsylvania State University. He obtained his PhD from University of Illinois at Urbana Champaign, MS from Duke University, and BA from Indian Institute of Technology Varanasi, all in Computer Science. His research interest is in the area of Internet of Things, with a focus on wireless networking and mobile sensing.

Ashutosh Dhekne received his MTech in Computer Science from Indian Institute of Technology Bombay. He is currently a PhD student at the University of Illinois at Urbana Champaign. He received the Richard T. Cheng Endowed Fellowship in 2014. His research interests are in the areas of wireless networking and mobile computing.

Sheng Shen is a PhD candidate in the Department of Electrical and Computer Engineering at the University of Illinois at Urbana Champaign. He received his BE from the University of Science and Technology of China in 2010. His research focuses on designing mobile systems with various sensors to analyze human mobility, simplify human-computer interaction and improving health.

Romit Roy Choudhury, a professor of ECE at the University of Illinois at Urbana Champaign, received his PhD from the Computer Science department at UIUC. His research interests are in wireless protocol design and mobile computing. He is a recipient of the 2017 ACM MobiSys Best Paper Award and the 2016 CS@UIUC Distinguished Alumni Award, among others.

Sharon Xue Yang holds a PhD in Computer Engineering from the University of Illinois at Urbana Champaign. She is a Principal Engineer at Intel New Technology Group, where she has been leading indoor localization technology and wearable sensing technology developments. She founded and co-chairs Bluetooth SIG coexistence working group, holds 130+ patents, and is the author of 30+ referred papers published in IEEE/ACM journals/conferences.

Lei Yang received his PhD from Univ. of California, Santa Barbara, and is presently a Senior Staff Engineer at Ant Financial Technology Labs working on IoT innovations. His areas of expertise include mobile computing, machine learning and wireless networking. He is a senior member of IEEE, has co-authored 20+ peer-reviewed technical papers and has 30+ issued or pending US patents.

Suresh Golwalkar is a principal engineer in Intel, Phoenix. He obtained his PhD from Rensselaer Polytechnic Institute.

Alexander Essanian works as a hardware design engineer at Intel, Santa Clara.

REFERENCES

- [1] D2m. <http://d2m-inc.com/>.
- [2] Ellipsoid or sphere fitting for sensor calibration. www.st.com/resource/en/design_tip/dm00286302.pdf
- [3] Hawk-eye. <https://en.wikipedia.org/wiki/Hawk-Eye>.
- [4] Inertial measurement unit. <https://stanford.edu/class/ee267/lectures/lecture9.pdf>
- [5] Motioncapturesystems-vicon. <https://www.vicon.com/>.
- [6] Motion sensors - android developers. https://developer.android.com/guide/topics/sensors/sensors_motion.html
- [7] PhaseSpace. <http://phasespace.com/>.
- [8] Artese, G., and Trecroci, A. “Calibration of a low cost mems ins sensor for an integrated navigation system.” *Int. Arch. Photogramm. Remote Sens. Spatial Inf. Sci* (2008), 877–882.
- [9] Cho, S. Y., and Park, C. G. “A calibration technique for a redundant imu containing low-grade inertial sensors.” *ETRI journal* 27, 4 (2005), 418–426.
- [10] Flenniken, W., Wall, J., and Bevly, D. “Characterization of various imu error sources and the effect on navigation performance.” In *Ion Gnss* (2005), pp. 967–978.
- [11] Gowda, M., Dhekne, A., Shen, S., Choudhury, R. R., Yang, X., Yang, L., Golwalkar, S., and Essanian, A. “Bringing IoT to sports analytics.” *Networked Systems Design and Implementation (NSDI)* 2017.

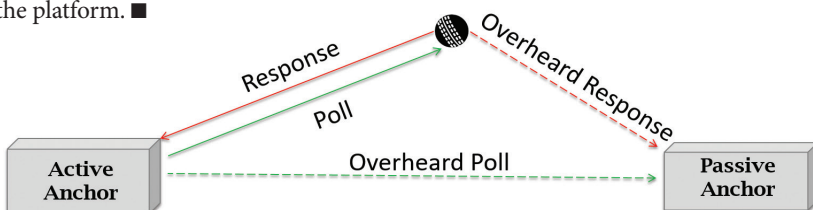


FIGURE 20. A passive anchor estimates its range from overheard poll/response packets.

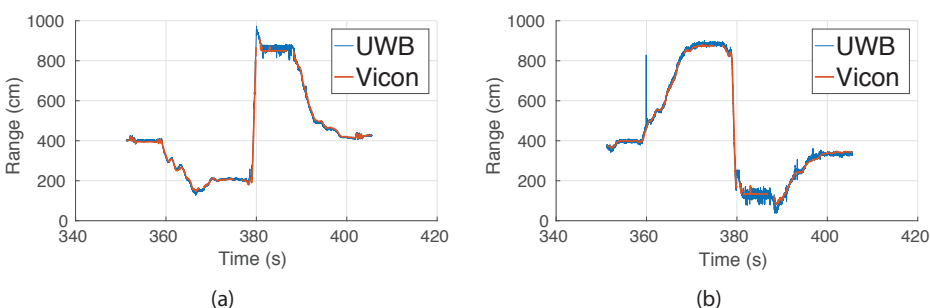


FIGURE 21. Similar to active ranging (a), passive ranging agrees with ViCON ground truth (b).